The huge influence of nanograins on the magnetic properties of iron-based Fe–Cu–Nb–B nanocrystalline alloys

2005 J. Phys.: Condens. Matter 17 3197

(http://iopscience.iop.org/0953-8984/17/21/014)

INSTITUTE OF PHYSICS PUBLISHING JOURNAL OF PHYSICS: CONDENSED MATTER

J. Phys.: Condens. Matter **17** (2005) 3197–3209 doi:10.1088/0953-8984/17/21/014

The huge influence of nanograins on the magnetic properties of iron-based Fe–Cu–Nb–B nanocrystalline alloys

H Bremers, O Hupe, C E Hofmeister, O Michele and J Hesse

Institut für Metallphysik und Nukleare Festkörperphysik, Technische Universität, Mendelssohnstrasse 3, D-38106 Braunschweig, Germany

E-mail: h.bremers@tu-bs.de

Received 20 December 2004, in final form 22 March 2005
Published 13 May 2005
Online at stacks.iop.org/JPhysCM/17/3197

Abstract

In 1995 Skorvanek and O'Handley presented the first experimental evidence for a huge influence of nanograins on the magnetization of a nanostructured alloy. In this contribution experiments are described, performed on as-cast amorphous and nanostructured $Fe_{79}Cu_1Nb_7B_{13}$ alloys. In order to get nanostructured samples with different nanograin contents the samples were annealed at different properly chosen temperatures in vacuum. This led to the formation of nanograins embedded in a residual amorphous matrix. These nanograins consist of pure bcc Fe of about 5–6 nm in diameter. Their content can be enhanced without markedly changing their size when annealing at slightly higher temperatures. So an alloy series with the same nominal composition but different nanograin contents and residual amorphous matrices, i.e. a series of nanostructured alloys, was obtained. Our aim was to study the influence of increasing nanograin concentration on the magnetic properties of the coupled system amorphous matrix plus nanograins. We describe magnetization measurements over a wide temperature range, below and above the Curie temperature of the initial amorphous matrix. In a next step these measurements are evaluated in a molecular field approach assuming two different coupled ferromagnetic systems assigned to the amorphous matrix and the nanograins.

1. Introduction

Modern nanostructured magnetic materials have been of interest to scientists and engineers for many years. It is surprising, considering the magnetic properties of nanostructured magnetic materials, that both extremely soft magnetic materials [1] (with applications in loss free transformers) and extremely hard magnetic materials [2] (with applications in permanent magnets) can be achieved. An overview of the physics and magnetism of such a system

was given by Hernando [3]. In this contribution we deal with an alloy of the FeCuNbB type which belongs to the family of soft magnetic materials.

After a suitable heat treatment, nanostructured ferromagnetic alloys of the FeCuNbB type consist of pure bcc iron nanograins embedded in an amorphous matrix. The presence of nanograins consisting of pure iron is advantageous for this alloy system. It allows one to estimate easily the large magnetic moment of the nanograins. In the Mössbauer spectroscopy the lineshape in the well known six-line pattern for bcc iron can be carefully investigated. This led to a new interpretation of Mössbauer spectra [4, 5] as regards thermal fluctuations of the magnetization in the nanograins. These nanograins are normally so small (typical diameter in the range 5–30 nm) that, if they were free, the thermal fluctuation of the magnetic moment would lead to superparamagnetic behaviour. Normally, as long as the temperature is lower than the Curie temperature of the initial amorphous matrix, the nanograins are coupled to the ferromagnetic matrix and a strong magnetic interaction between these two components must be considered. This determines the thermally driven fluctuation of the nanograin magnetic moments and leads to a huge influence on the resulting magnetization when increasing the nanograin concentration.

This dramatic influence becomes visible when the temperature of the sample is enhanced over the Curie temperature of the initial amorphous matrix. Here it is evident that we observe a unique new magnetic behaviour which results from the two magnetically interacting but, from their structure, easy to distinguish different phases—the residual amorphous matrix and the nanograins. This magnetic behaviour we call 'two-phase superferromagnetism' extending the term superferromagnetism which was first introduced by Morup *et al* [6] for nanoparticle systems. In their pioneering study on goethite nanosystems the particles touch each other, so providing a way for the exchange interaction to occur. In the case of our investigation transmission electron microscopy (TEM) results show well separated nanoparticles. Therefore the second phase, the residual amorphous matrix, is necessary for transmitting the nanograin–nanograin interactions.

Skorvanek and O'Handley [7] presented previously a very similar study increasing the content of nanograins in a $Fe_{72}Cu_1Nb_{4.5}Si_{13.5}B_9$ alloy by successive enhancements of the annealing temperature. Performing magnetization measurements, they have shown that increasing interparticle interaction suppresses superparamagnetic fluctuations of the single nanograins and leads to collective magnetic behaviour. The measurements of Skorvanek and O'Handley were performed in one external magnetic field $B_{\mathrm{ext}} = 1$ T only.

In this contribution we report on magnetization measurements performed on ferromagnetic $Fe_{79}Cu_1Nb_7B_{13}$ alloys with different nanograin contents in various external magnetic fields.

2. The alloy samples and magnetization measurements

The amorphous alloy ribbons were produced by the Vacuumschmelze GmbH, Hanau, Germany, and were provided by Dr G Herzer. The thickness of the long ribbons is about 24 μm and their width 14.8 mm. One very important feature of the system in question is that the nanocrystallites appearing after suitable annealing consist of pure bcc Fe about 5–6 nm in diameter. The samples were annealed in vacuum always for one hour at the temperatures indicated. The suitable annealing temperatures we found by differential scanning calorimetry (DSC). Figure 1 shows a typical DSC measurement on a $Fe_{79}Cu_1Nb_7B_{13}$ alloy. From this the annealing temperatures indicated by perpendicular lines were chosen. Each sample was annealed in vacuum for one hour at the temperatures indicated by the letters J, I, E, F, ... We used small parts of the ribbons formed as 5 mm diameter circles or 5×5 mm^2 squares as samples for magnetization measurements. The external magnetic field is applied parallel to the ribbon plane. This different

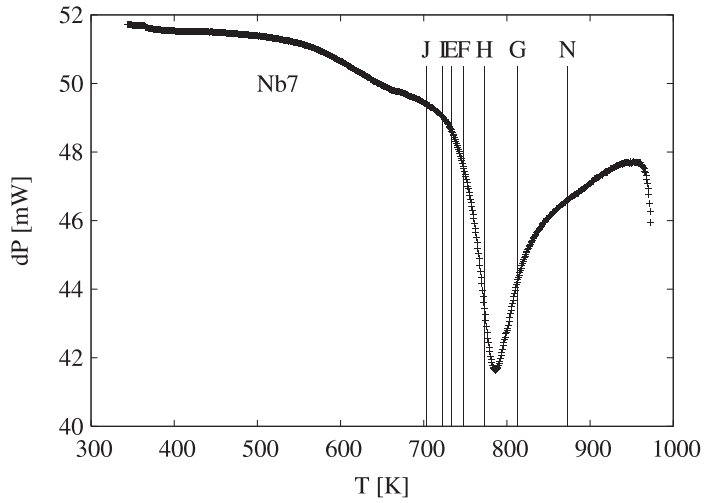

Figure 1. A typical DSC measurement on the $Fe_{79}Cu_1Nb_7B_{13}$ alloy. From this DSC scan the annealing temperatures indicated by perpendicular lines were chosen. The letters J, I, E, F, ... indicate different annealing temperatures.

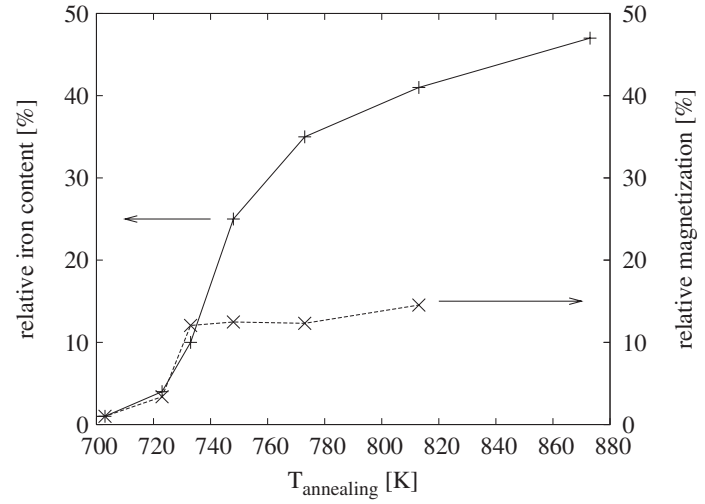

Figure 2. The relative content of iron in the annealed $Fe_{79}Cu_1Nb_7B_{13}$ alloy samples versus annealing temperature as derived from room temperature Mössbauer spectra presented in figure 3. Additionally the dashed curve shows the relative part of the nanograin magnetization of the samples as determined by fitting the model described to the magnetization.

annealing temperature leads to different amounts of nanocrystallites. These nanograins are of nearly the same size exhibiting a rather narrow size distribution and are well separated from each other. This fact has been checked using transmission electron microscopy [8, 9].

Additionally we used the fact that the nanograins consist of pure bcc iron. So it becomes possible to measure the relative amount of the iron bcc component assigned to the nanograins in comparison to the remaining iron belonging to the amorphous phase and nanograin interface from the area of the corresponding ^{57}Fe Mössbauer spectra.

Figure 2 presents the growing content of iron in the nanograins as derived from room temperature Mössbauer spectra. Combining these results with transmission electron

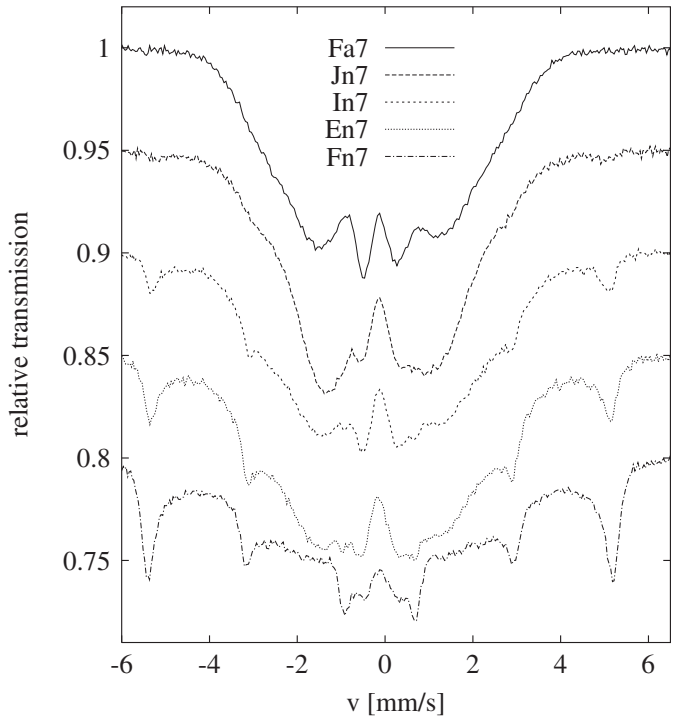

Figure 3. Mössbauer spectra collected at room temperature for the $Fe_{79}Cu_1Nb_7B_{13}$ alloy samples annealed at the temperatures labelled J, I, E, F. Fa represents the spectrum of the initial amorphous alloy. The spectra are shifted downwards for better representation.

Table 1. Grain sizes of the samples.

Alloy	En7	Fn7	Hn7	Gn7	Nn7
Annealing temperature	733	748	773	813	873
Mean grain diameter (nm)	5.6	5.4	7*	7	7.4
Width of norm. log dist. (nm)	0.9	0.8	—	—	1.5
Estimated grain distance (nm)	6	3.3	2.9	2.4	2.2

microscopy the conclusion could be drawn that for the samples J to H to a very good approximation the number of nanograins is increasing with annealing temperature whereas their sizes and size distribution remain nearly the same. The mean distance between the nanoparticles decreases with increasing annealing temperature. From transmission electron microscopy the following data summarized in table 1 were obtained. The mean grain distance was estimated by the Hernandos *et al* formula [10] using the grain diameters from TEM and x-ray diffraction (using the Warren–Averbach approach, marked with *) and the relative part of iron in the nanograins determined by Mössbauer spectroscopy.

We performed the magnetization measurements in a vibrating sample magnetometer (VSM, Oxford Instruments VSM 1.2H/CF/HT) in the temperature range starting from room temperature (300 K) and going up to about 700 K. It was necessary to limit the highest temperature to a value for which no further crystallization (either nanograin production or growth) or microcrystallization takes place. To be sure that the samples were not changed due to the measurements being at higher temperatures we collected Mössbauer spectra before and after each measurement at room temperature and compared them carefully.

A second step must also be mentioned. For each sample (i.e. for each alloy with a defined nanograin content) we performed many magnetization measurements applying external magnetic fields B_{applied} ranging from typically 10 to 1000 mT. We made the experience when applying smaller fields the samples were sometimes not magnetically saturated, i.e. they probably exhibited a domain structure, which leads to a misinterpretation of the magnetization results. Also, possible influences of the nanograin interface discussed later may cause such effects. In a high enough external field the sample is single domain. A further essential fact is that the (ferro)magnetism of the samples is due to the local magnetic iron moments alone. Iron is a constituent of the residual amorphous phase and of the nanograins. When the nanograin concentration is enhanced due to annealing at higher temperatures the iron content in the residual amorphous matrix becomes lower. This will change for example the formally introduced Curie temperature of the residual amorphous phase.

3. Measurement evaluation

To describe the magnetization over the whole temperature range and at different applied external magnetic fields some basic assumptions should be made. In this work the molecular field approximation is used. The magnetization in an external field B of a single-phase homogeneous ferromagnet then reads $M(T, B)$ and will be given by the transcendental equation with the Brillouin function B_S on the right. The spin of the atoms determining the thermal behaviour of the magnetization is S. The molecular field constant λ in the molecular field $B_{\text{MOL}} = \lambda M(T)$ was replaced by the Curie temperature T_{C}:

$$M(T, B) = M(0) B_S \left[\left(\mu \frac{3ST_{\text{C}}k_{\text{B}}}{(S+1)\mu M(0)} M(T) + \mu B \right) \frac{1}{k_{\text{B}}T} \right]$$

$$T_{\text{C}} = \frac{\lambda \mu M(0)(S+1)}{3k_{\text{B}}S}.$$

The other symbols are: k_{B}, the Boltzmann constant; μ_{B}, the Bohr magneton; $M(0)$, the saturation magnetization; and μ, the maximal magnetic moment $\mu = \mu_{\text{B}} g_S S$ of the atoms with g_S the g-factor.

In our experiments we measured the magnetization M_{Mass} with respect to the sample mass m_{Sample}, not to the volume V. Therefore for the volume related magnetization, here the saturation value $M(0)$, the relation

$$M(0) = \frac{N_{\text{Atom}}\mu}{V} = \frac{N_{\text{Atom}}\,\mu}{m_{\text{Sample}}} \frac{m_{\text{Sample}}}{V} = M_{\text{Mass}}(0)\rho$$

holds, were ρ means the density of the sample material and N_{Atom} is the number of spin carrying atoms in the sample. If there is no unexceptional volume expansion we can assume approximately that over the whole temperature range

$$\frac{\rho(T)}{\rho(0)} \approx 1.$$

In nanostructured alloys this spin value can be very large because it must be assigned to the collective behaviour of 'spin clusters' forming the nanograins. The term $\mu B = (g_S \mu_{\text{B}} S)B$ in the argument of the Brillouin function is the one sensitive enough for these influences. Due to this term, for nanoparticles with large spin the course of the magnetization near T_{C} is influenced significantly and so allows a sensitive determination of the nanograin spin value in question.

In an alloy composed from many different atoms with only one atom kind carrying a magnetic moment, we assign to each magnetic atom a mean atomic $\overline{m}_{\text{Atom}}$ mass, being a

consequence of this composition. For example the gross composition of the amorphous $Fe_{79}Cu_1Nb_7B_{13}$ alloy leads to a mean atomic mass (which must be assigned to each iron atom in order to determine the corresponding saturation magnetization $M_{\mathrm{Mass}}(0)$)

$$100\overline{m}_{\mathrm{Atom}} = 79m_{\mathrm{Fe}} + 1m_{\mathrm{Cu}} + 7m_{\mathrm{Nb}} + 13m_{\mathrm{B}}.$$

Assuming that we have $N_{\mathrm{A}} = 6.023 \times 10^{23}$ (the Avogadro number) of Fe atoms in the sample or one mole of Fe atoms, we find

$$\overline{m}_{\mathrm{Atom}}(Fe_{79}Cu_1Nb_7B_{13}) = 52.66 \text{ g mol}^{-1}.$$

It makes sense to introduce the mass–spin ratio $X_{\mathrm{Mass-Spin}}$:

$$X_{\mathrm{Mass-Spin}} = \frac{\overline{m}_{\mathrm{Atom}}}{S_{\mathrm{Atom}}}; \qquad M_{\mathrm{Mass}}(0) = \frac{N_{\mathrm{Atom}} g_S \mu_{\mathrm{B}}}{N_{\mathrm{Atom}}} \frac{S_{\mathrm{Atom}}}{\overline{m}_{\mathrm{Atom}}} = \frac{g_S \mu_{\mathrm{B}}}{X_{\mathrm{Mass-Spin}}}$$

where N_{Atom} is the number of atoms carrying a magnetic moment.

For bcc iron the mass related saturation magnetization is 220 emu g^{-1} which corresponds to 220 A m^2 kg^{-1}. From that, the magnetic moment for an iron atom follows: $\mu_{\mathrm{Fe}} = 2.2\ \mu_{\mathrm{B}}$. Assuming $g_S = 2$, the effective spin value of $S_{\mathrm{Fe}} = 1.1$ follows. From these values we find, assuming one mole of iron atoms, $(X_{\mathrm{Mass-Spin}})_{\mathrm{bcc\,Fe}} = m_{\mathrm{Fe}}/S_{\mathrm{Fe}} = 50.77 \text{ g mol}^{-1} \approx 51 \text{ g mol}^{-1}$.

Next we consider the alloy $Fe_{79}Cu_1Nb_7B_{13}$. For the as-quenched amorphous matrix (without nanograins) we measured the magnetization saturation value of 136 emu g^{-1}, or 136 A m^2 kg^{-1}. In comparison to the case for pure bcc iron, assuming again one mole of iron atoms, the formally introduced effective spin assigned to each atom must be lower. Here we find $S_{\mathrm{Fe\,amorphous}} = 0.83$. So for the as-quenched amorphous matrix the mass–spin ratio is $(X_{\mathrm{Mass-Spin}})_{\mathrm{amorph\,Fe}} = 82.14 \text{ g mol}^{-1}$. Considering nanostructured alloys with increasing concentration of nanograins we expect $(X_{\mathrm{Mass-Spin}})_{\mathrm{amorph\,Fe}}$ to start to increase because the mean mass assigned to one iron atom in the residual amorphous phase will increase too. In the further treatment $(X_{\mathrm{Mass-Spin}})_{\mathrm{amorph\,Fe}}$ therefore becomes one of the parameters to be fitted.

4. Two-phase superferromagnetism

Here we present a model describing the magnetization of two magnetically coupled ferromagnetic phases. The amorphous matrix is regarded as one ferromagnetic phase (1) and the nanograins embedded into this matrix as the second ferromagnetic phase (2). Then the magnetization (here first with respect to the volume) of the system reads

$$M(T) = M_1(T) + M_2(T)$$
$$M_{\mathrm{Mass}}(T)\rho = M_{1\ \mathrm{Mass}}(T)\rho_1 + M_{2\ \mathrm{Mass}}(T)\rho_2.$$

Again ρ denotes the density of the alloy and its phases (1) and (2) respectively. For the mass related saturation magnetization, it follows that

$$M_{1\ \mathrm{Mass}}(0) = \frac{(1-\alpha)g_S\mu_{\mathrm{B}}}{X1_{\mathrm{Mass-Spin}}}; \qquad M_{2\ \mathrm{Mass}}(0) = \frac{\alpha g_S \mu_{\mathrm{B}}}{X2_{\mathrm{Mass-Spin}}}$$

with α the relative contribution of the nanograin magnetization. For both 'partial' magnetizations we make the ansatz

$$\frac{M_{1\ \mathrm{Mass}}(T)}{M_{1\ \mathrm{Mass}}(0)} = B_{S1}\left(\left(\frac{3S_1}{(S_1+1)M_{1\ \mathrm{Mass}}(0)}(T_{\mathrm{C1}}\, M_{1\ \mathrm{Mass}}(T) + T_{\mathrm{K1}}\,\frac{\rho_2}{\rho_1} M_{2\ \mathrm{Mass}}(T)) + \frac{g_S\mu_{\mathrm{B}}}{k_{\mathrm{B}}} S_1 B\right)\frac{1}{T}\right) \tag{1}$$

$$\frac{M_{2\ \mathrm{Mass}}(T)}{M_{2\ \mathrm{Mass}}(0)} = B_{S2}\left(\left(\frac{3S_2}{(S_2+1)M_{2\ \mathrm{Mass}}(0)}(T_{C2}M_{2\ \mathrm{Mass}}(T) + T_{K2}\frac{\rho_1}{\rho_2}M_{1\ \mathrm{Mass}}(T)) + \frac{g_S\mu_B}{k_B}S_2B\right)\frac{1}{T}\right). \quad (2)$$

So we obtain a system of two transcendental equations describing the magnetization of the different coupled phases, amorphous (1) and nanograin (2).

In the argument of the Brillouin function B_{S1} we find the Curie temperature T_{C1} of the amorphous phase (1), with atoms (or small atomic clusters) carrying the spin S_1, and in the argument of the Brillouin function B_{S2} the temperature T_{C2} of phase (2) which is the Curie temperature of the coupled nanograin system, i.e. particles carrying the large spin S_2. On both kinds of magnetic moments there acts the external magnetic field B. Both phases are coupled. This coupling is again expressed via an additional molecular field which phase (1) causes on phase (2) and vice versa. This molecular field is in our model assumed to be proportional to the magnetization of the other phase. Again we express the coupling strength using a formal temperature, here T_{K1} and T_{K2} respectively. So for example we set as a definition for the coupling temperature T_{K1} expressing the influence of the magnetization of phase (2) on the magnetization on phase (1)

$$\mu_1\lambda_2M_2(T) = T_{K1}\frac{3k_BS_1}{(S_1+1)}\frac{M_2(T)}{M_1(0)} = T_{K1}\frac{3k_BS_1}{(S_1+1)}\frac{\rho_2M_{\mathrm{Mass},2}(T)}{\rho_1M_{\mathrm{Mass},1}(0)}.$$

Because ρ_1 and ρ_2 are expected to be not very different we consider $T^*_{K1} = T_{K1}\rho_2/\rho_1$ and $T^*_{K2} = T_{K2}\rho_1/\rho_2$ as two independent fitting parameters. In the following we will not distinguish between T_K and T^*_K. Thus the two coupled phases exhibit a common Curie temperature which is a function of all the four parameters T_{C1}, T_{C2}, T_{K1}, T_{K2} expressed as temperatures appearing in the arguments of the Brillouin function. This dependence can be found by expanding the Brillouin function for small arguments in the neighbourhood of T_{Curie}:

$$(T_{\mathrm{Curie}} - T_{C1})(T_{\mathrm{Curie}} - T_{C2}) = T_{K1}T_{K2}.$$

Our ansatz also contains the case when the nanograins are not coupled to the residual amorphous matrix. In that case, $T_{K2} = 0$, the nanograin phase (2) behaves superparamagnetically above T_{C1}.

So fitting the above equations to measured magnetization curves in a given external magnetic field, the following parameters must be determined:

$$S_1,\ S_2, T_{C1}, T_{C2}, T_{K1}, T_{K2}, M_{1\ \mathrm{Mass}}(0),\ M_{2\ \mathrm{Mass}}(0)$$

but instead of the last saturation magnetization we fitted

$$\alpha \text{ and } X1_{\mathrm{Mass-Spin}} = \frac{\overline{m}_{\mathrm{Atom}}}{S_{\mathrm{Atom}}}.$$

$X2_{\mathrm{Mass-Spin}} = 51\ \mathrm{g\ mol^{-1}}$ was assumed to have the value of bulk iron. Because this is a minimal necessary but rather large number of parameters for describing the magnetic behaviour of the two coupled magnetic phases, we performed measurements in many different external magnetic fields and tried to fit all these results with a common set of parameters valid for all fields applied.

4.1. Fitting details

Because the measurements cover a rather large temperature range we have to correct for the effect of the ferromagnetism 'inside' the nanograins, i.e. the influence of internal excitations. Considering one nanograin we assume that its magnetization 'inside' behaves like the bulk iron

one. Therefore the nanoparticle changes its properties like saturation magnetization $M_{2\mathrm{Mass}}(0)$ and also the corresponding spin value S_2 with temperature.

To calculate the thermal expectation value $S_2(T)$ for the spin of the iron atoms 'inside' the nanograins we use the well known effective value $S_{\mathrm{Fe}} = 1.1$ and the Curie temperature for bulk iron $T_{\mathrm{C,Fe}} = 1043$ K:

$$S_2(T) = S_2(0)\, B_{\mathrm{S,Fe}}\left(\frac{3 S_{\mathrm{Fe}} S_{\mathrm{Fe}}(T)}{(S_{\mathrm{Fe}}+1)}\frac{T_{\mathrm{C,Fe}}}{T}\right).$$

The value $S_2(T = 0) = S_2$ is determined by the size of the nanograin and is one of the parameters to be fitted, too.

4.2. Demagnetizing field

For the magnetic field B experienced by the sample a small demagnetization correction must be done:

$$B = B_{\mathrm{applied}} - B_{\mathrm{demagnet}}(T) = B_{\mathrm{applied}} - \mu_0 N M(T).$$

The demagnetizing factor N for our samples we estimated to be $N = 0.05$ (μ_0 is the magnetic field constant).

5. Results from magnetization measurements

From the fits to the magnetization curves taken for one nanostructured alloy for all applied external magnetic fields, the parameters described in the model are obtained. It follows that the formal Curie temperature of the remaining amorphous phase T_{C1} becomes lower with decreasing Fe content (i.e. increasing content of bcc Fe nanograins). Superparamagnetic behaviour of the nanograins is observed for the $Fe_{79}Cu_1Nb_7B_{13}$ annealed at 703 and 723 K. The first evidence for particle–particle interaction appears for the sample annealed at 733 K. It becomes more obvious for the sample annealed at 748 K. Two-phase superferromagnetic behaviour (forced by the external magnetic field) is also observed for the samples annealed at 773 and 813 K). The parameter α describing the contribution of the nanograin magnetization relative to the total magnetization of the system shows qualitatively the same dependence as the relative part of iron atoms belonging to the nanograin phase (figure 2).

5.1. Magnetization of the amorphous alloy

First we present the magnetization curves for the amorphous alloy before annealing. We used the as-quenched sample and measured the magnetization in different magnetic fields (for examples see figure 4) for the magnetic field parallel to the ribbon plane but also parallel to the rolling direction and perpendicular to it. There was no significant difference between these two measurements.

Our program was able to fit all curves for all applied magnetic fields simultaneously. Results are summarized in table 2.

Starting with these results gained for the amorphous alloys, the magnetization curves for the nanostructured alloys were fitted. The model parameters obtained are summarized in table 3. In this table a systematic decrease of T_{C1} is observed. T_{C1} is the formal Curie temperature of the residual amorphous matrix. This can be expected because in our system iron is the only atom carrying a magnetic moment and its content decreases with increasing nanograin component.

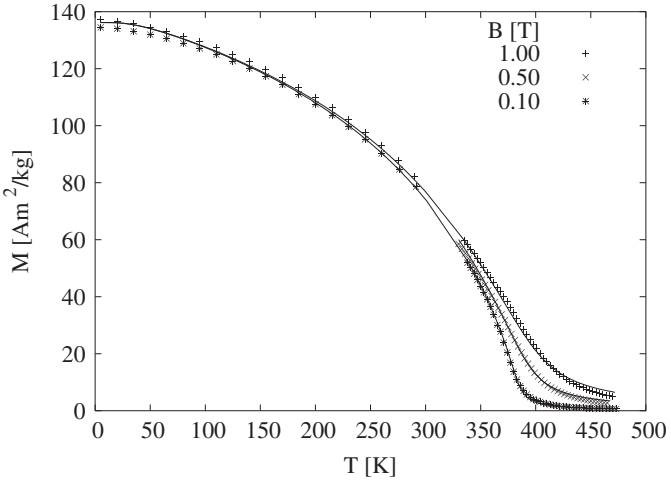

Figure 4. The magnetization versus temperature for the amorphous $Fe_{79}Cu_1Nb_7B_{13}$ alloy in three different external magnetic fields.

Table 2. Parameters obtained for the amorphous alloy.

B (T)	T_C (K)	S	X (g)	M_0 (A m^2 kg^{-1})
0.1, 0.5, 1.0	352	9.2	82.3	136

Table 3. Parameters applied to describe the magnetization curves.

T_a (K)	α (1)	S_1 (1)	S_2 (1)	T_{C1} (K)	T_{C2} (K)	$X1$ (g mol^{-1})	$X2$ (g mol^{-1})	T_{K1} (K)	T_{K2} (K)	M_0 (A m^2 kg^{-1})
703	0.01	10.4	6 500	378	0	82	51	168	0	137
723	0.03	10.5	7 650	372	140	84	51	165	35	137
733	0.12	11.5	13 700	360	590	87	51	124	127	139
748	0.12	10.8	13 600	311	520	86	51	266	340	141
773	0.12	10.5	9 400	191	700	85	51	653	628	142
813	0.14	10.5	43 000	117	780	86	51	839	772	143

With this set of parameters it becomes possible to simulate the spontaneous magnetization curves of the two-phase superferromagnets for different contents of nanograins in all not too low magnetic fields applied. Examples are given in figures 5 and 6. All fitting parameters are summarized in table 3 ($X2$ is calculated as described in the text). Additionally the magnetization of the two-phase superferromagnet can be obtained for a vanishing external field. To do this we approximated the value $B = 0$ by $B = 0.001$ mT. The result (not obtainable by a measurement) is shown in figure 7. The slightly different values of the saturation magnetization values are adapted from our low temperature magnetization measurements, showing that in real alloys there is a weak dependence of the magnetic moments of the iron atoms on their surroundings.

6. Summary and discussion

We presented experimental investigations on alloys consisting of bcc Fe nanograins embedded in a ferromagnetic residual amorphous matrix. The samples were achieved by suitable

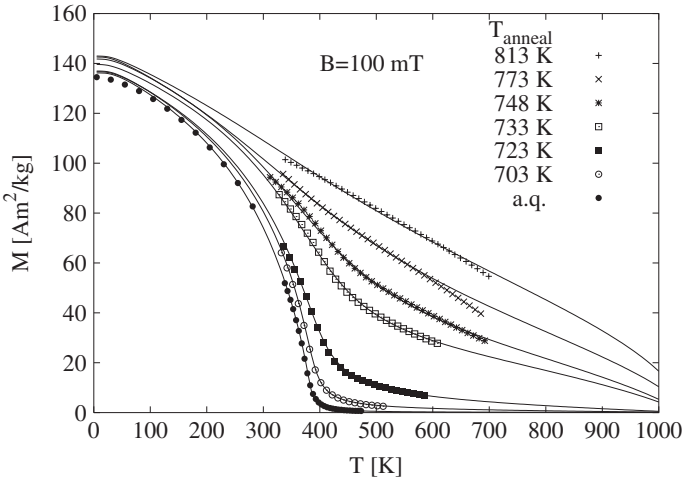

Figure 5. Result of magnetization measurements versus temperature performed in an external magnetic field of 100 mT for the $Fe_{79}Cu_1Nb_7B_{13}$ alloy samples annealed at the temperatures indicated in the figure together with the fit achieved using the model described in the text. a.q. represents the as-quenched state of the amorphous alloy.

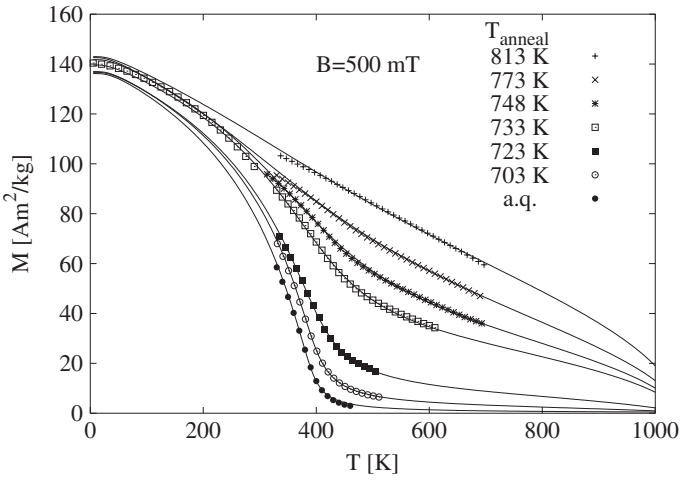

Figure 6. Result of magnetization measurements versus temperature performed in an external magnetic field of 500 mT for the $Fe_{79}Cu_1Nb_7B_{13}$ alloy samples annealed at the temperatures indicated in the figure together with the fit achieved using the model described in the text. a.q. represents the as-quenched state of the amorphous alloy.

annealing of the initial amorphous $Fe_{79}Cu_1Nb_7B_{13}$ alloy at different temperatures as found by DSC measurements. Mössbauer spectrometry and TEM delivered additional information about the iron content in the bcc nanograins and nanograin sizes as well as size distributions. The main topic was magnetization measurements performed on numerous samples of nanostructured alloys over a large range of external magnetic fields. These measurements clearly demonstrated a huge influence of the nanograins on the magnetic behaviour of the whole system as first reported by Skorvanek and O'Handley [7]. We called this collective magnetic behaviour of nanograins coupled with and through the residual amorphous matrix 'two-phase superferromagnetism' extending the idea of superferromagnetism first introduced by Morup

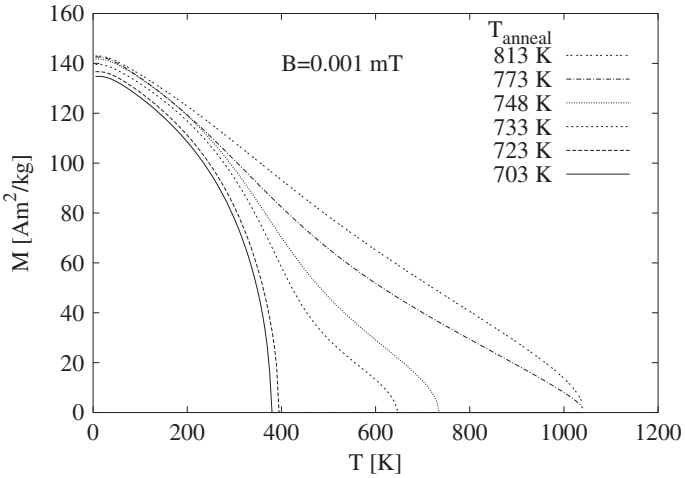

Figure 7. Result of calculation using the model presented for zero magnetic field ($M = 0.001$ mT) with parameters from table 3. This plot shows the behaviour of the spontaneous magnetization of the two-phase superferromagnet and covers temperature ranges above the crystallization temperature of the samples.

et al [6] for nanograins in direct contact with each other. The nanograins in the system described here are clearly separated from each other as evidenced by TEM investigations. Therefore any particle–particle interaction must be transmitted via the residual amorphous matrix. The name 'two-phase superferromagnetism' results from the fact that it is easy to distinguish two metallurgically different phases—the crystalline nanograins and the amorphous residual matrix, but in the sense of collective magnetism there is only one phase when the nanograin content is high enough (within our model, i.e. $T_{K2} \neq 0$). At very low nanograin concentration the magnetization delivers evidence for superparamagnetic behaviour of the nanograins above the Curie temperature of the amorphous phase. This can be evidenced by plotting magnetization curves taken at different temperatures versus B/T [11]. At higher nanograin concentration a characteristic change in the magnetization curves is observed: the separate Curie temperature of the amorphous ferromagnetic component vanishes and the collective magnetic behaviour of the two phases appears in total agreement with the experiments of Skorvanek and O'Handley [7, 12] performed on $Fe_{72}Cu_1Nb_{4.5}Si_{13.5}B_9$.

In order to describe this collective magnetic behaviour of the two coupled phases a model based on the molecular field idea was proposed and fitted to the magnetization measurements. In this model the origin of this collective magnetic behaviour is to be seen in the magnetic interactions of the nanograins with each other and with the residual amorphous matrix. First each phase (amorphous and nanocrystalline) is treated formally as a ferromagnet with its own Curie temperature and corresponding molecular field. The interactions between the phases are expressed via additional molecular fields, similar to the well known description of antiferromagnetism or ferrimagnetism in crystalline systems. As usual the molecular field interpretation does not give any explanation of the microscopic mechanism of the intergrain coupling via the residual amorphous matrix. In our model the existence and influence of the nanograin interface is completely neglected. Very detailed interpretation of Mössbauer spectra and corresponding hyperfine field distributions published by Miglerini and Greneche [13] evidenced the role and structure of the interface of the nanograins. In addition to the well established ideas about the exchange interactions at and through the grain boundaries called

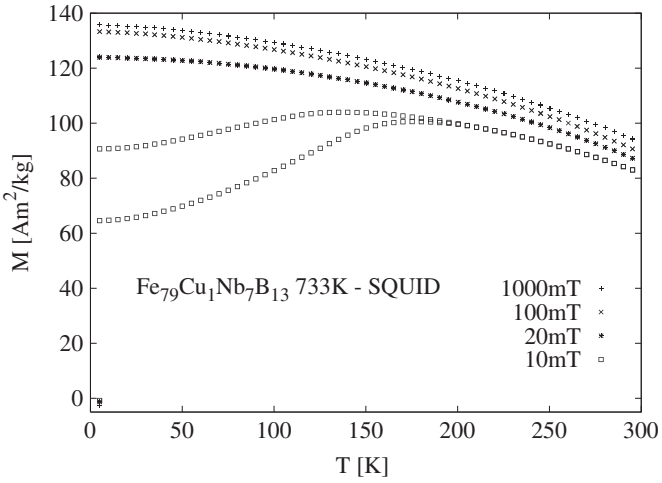

Figure 8. Presented are magnetization measurements performed on the nanostructured sample $Fe_{79}Cu_1Nb_7B_{13}$ annealed at 733 K in the magnetic fields indicated. The lowest curve measured in 10 mT was achieved after zero-field cooling. The second lower curve was also measured in 10 mT after field cooling in 10 mT.

interfaces [6, 7] we would like to propose considering also the transmission of the dipole–dipole nanograin interaction 'enhanced' by the high magnetic polarizability of a ferromagnetic matrix (here our residual amorphous one) above its Curie temperature. How such a dipole–dipole interaction (and its strength distribution) can lead to a new interpretation of Mössbauer spectra collected on nanoparticles in such systems was recently described by Afanas'ev and Chuev [5] and used by Hupe *et al* [9] to interpret experimental results.

The problem of interparticle interactions in nanoparticle assemblies has been discussed many times [14, 3]. In our molecular field model the existence and experimentally evidenced influence of the nanograin interface cannot be treated. So the validity of the model described is limited to not too low magnetic fields. Nevertheless the nanograin interface influence is present also in our experiments. We observe an anomaly in the behaviour of the magnetization measured in low external magnetic fields when starting at low temperatures. One typical example is presented in figure 8 which shows field warming magnetization measurements after zero-field cooling (ZFC) and field cooling (FC) in different external magnetic fields.

Here it is observed that in a low enough external magnetic field (10 mT) after ZFC the FW magnetization first increases with temperature and that this increase is stronger than that observed after FC and FW. On increasing the external field strength this effect disappears. In external fields bigger then 20 mT this influence vanishes step by step and the saturation magnetization for all samples can be achieved. This behaviour can be interpreted as a consequence of the interface influence. The interface of the nanoparticles due to the complex magnetic structure seems to be able to tilt the magnetic moment of the nanoparticles from the parallel direction offered by the external magnetic field. Such influences were reported, observing the increase of coercivity at low temperatures, by Skorvanek *et al* [15, 16]. The authors relate this behaviour and also the observed creep to magnetic moments of the nanocrystalline grains and highly distorted interfaces frozen in their random anisotropy orientations.

We succeeded in fitting the model presented directly to the magnetization measurement results and determined the parameters in question. Our experience is that although fitting

simultaneously magnetization measurements performed in many different external magnetic fields the model parameters can only be obtained with some uncertainty but with clear identification of the very large spin of the nanograins. From our experiments we learned that a minimal strength of the external magnetic field is necessary to avoid interface effects. So typically the lowest field applied should be of the order of 100 mT.

Acknowledgments

Our thanks go to Dr K Weyand and H Ahlers, Physikalisch-Technische Bundesanstalt, Braunschweig, for allowing us access to the SQUID magnetometer facility in their laboratory and to our colleagues at the University of Thessaloniki (Greece), Professors Dr K Efthimiadis and Prof Dr E K Polychroniadis, for performing the TEM investigations. We are grateful to Dr G Herzer for providing us with the amorphous samples. We are also grateful to the Deutsche Forschungsgemeinschaft for supporting the experimental work within the project He1025/11-2,3.

References

[1] Herzer G 1993 *Phys. Scr.* T **49A** 307–14
[2] Seeger M and Kronmüller H 1996 *Z. Metallk.* **87** 923–33
[3] Hernando A 1999 *J. Phys.: Condens. Matter* **11** 9455–82
[4] Chuev M A, Hupe O, Afanas'ev A M, Bremers H and Hesse J 2002 *JETP Lett.* **76** 558–62
[5] Afanas'ev A M and Chuev M A 2001 *JETP Lett.* **74** 107–10
[6] Morup S, Madsen M B and Franck J 1983 *J. Magn. Magn. Mater.* **40** 163–74
[7] Skorvanek I and O'Handley R C 1995 *J. Magn. Magn. Mater.* **140–144** 467–8
[8] Hesse J, Hupe O, Hofmeister C E, Bremers H, Chuev M A and Afanas'ev A M 2002 *Material Research in Atomic Scale by Mössbauer Spectroscopy (NATO Advanced Research Workshop, June 2002)* pp 117–27
[9] Hupe O, Chuev M A, Bremers H, Hesse J, Afanas'ev A M, Efthimiadis K G and Polychroniadis E K 2002 *Material Research in Atomic Scale by Mössbauer Spectroscopy (NATO Advanced Research Workshop, June 2002)* pp 137–47
[10] Hernando A, Navarro I and Gorria P 1995 *Phys. Rev.* B **51** 3281–4
[11] Hupe O 2003 *PhD Thesis* Cuvillier Verlag Göttingen (ISBN 3-89873-628-8)
[12] Skorvanek I, Kim C K and O'Handley R C 1995 *Science and Technology of Rapid Solidification Process* (Dordrecht: Kluwer) pp 309–16
[13] Migelerini M and Greneche J-M 1999 *Hyperfine Interact.* **121** 297–301
[14] Dormann J L, Fiorani D and Tronc E 1999 *J. Magn. Magn. Mater.* **202** 251–67
[15] Skorvanek I, Kovac J and Kötzler J 2003 *Phys. Status Solidi* **236** 303–9
[16] Skorvanek I, Skwirblies S and Kötzler J 2001 *Phys. Rev.* B **64** 184437